R.A.1295

NACA

RESEARCH MEMORANDUM

for the

Bureau of Aeronautics, Navy Department

EFFECTS OF VARIATIONS IN FOREBODY AND AFTERBODY DEAD RISE ON THE

RESISTANCE AND SPRAY CHARACTERISTICS OF THE 22ADR CLASS

VPB AIRPLANE - LANGLEY TANK MODEL 207

TED NO. NACA 2361

By

Eugene P. Clement and Charles J. Daniels

Langley Memorial Aeronautical Laboratory
Langley Field, Va.

NATIONAL ADVISORY COMMITTEE
FOR AERONAUTICS

WASHINGTON

AUG 28 1947

NATIONAL ADVISORY COMMITTEE FOR AERONAUTICS

RESEARCH MEMORANDUM

for the

Bureau of Aeronautics, Navy Department

EFFECTS OF VARIATIONS IN FOREBODY AND AFTERBODY DEAD RISE ON THE

RESISTANCE AND SPRAY CHARACTERISTICS OF THE 22ADR CLASS

VPB AIRPLANE - LANGLEY TANK MODEL 207

TED NO. NACA 2361

By Eugene P. Clement and Charles J. Daniels

SUMMARY

An investigation was made to determine the effects of changes in the amount and distribution of forebody and afterbody dead rise on the hydrodynamic resistance and spray characteristics of a $\frac{1}{11}$-size model of the Bureau of Aeronautics design No. 22ADR class VPB airplane. The variations in dead rise within the range investigated had no significant effects on resistance or trim, free to trim, or on resistance or trimming moment, fixed in trim. The coordinates of the peaks of the bow-spray blisters, with reference to the model, were measured at low speeds, and it was found that the model with the low dead rise at the bow had the lowest blisters. The changes in position of the maximum dead rise of the afterbody had no effect on the bow-spray blister.

INTRODUCTION

The results of resistance and spray tests of a $\frac{1}{11}$-size model of the Bureau of Aeronautics design No. 22ADR, class VPB airplane (Langley tank model 207) have been reported in reference 1. An additional investigation has been made to evaluate the effects of changes in the amount and distribution of the forebody and afterbody dead rise on the resistance and spray characteristics. This investigation was requested by the Bureau of Aeronautics, Navy Department. Five combinations of three forebodies (which differed in the amount of dead rise at the bow)

and three warped afterbodies (which differed in the position of maximum dead rise) were tested, and the results are presented in this report.

SYMBOLS

C_Δ load coefficient $\left(\dfrac{\Delta}{wb^3}\right)$

C_{Δ_0} gross-load coefficient $\left(\dfrac{\Delta_0}{wb^3}\right)$

C_V speed coefficient $\left(\dfrac{V}{\sqrt{gb}}\right)$

C_R resistance coefficient $\left(\dfrac{R}{wb^3}\right)$

C_M trimming-moment coefficient $\left(\dfrac{M}{wb^4}\right)$

C_L aerodynamic lift coefficient $\left(\dfrac{\text{Lift}}{\frac{1}{2}\rho SV^2}\right)$

τ trim, degrees (angle between forebody keel at the step and the water plane)

where

w maximum beam at chines, feet

Δ load on water, pounds

Δ_0 gross load, pounds

V carriage speed, feet per second

g acceleration of gravity, feet per second per second

R resistance, pounds

M trimming moment, pound-feet

S area of wing, square feet

ρ   density of air, slugs per cubic foot

w   specific weight of water, pounds per cubic foot (63.4 for
these tests; usually taken as 64 for sea water)

DESCRIPTION OF MODEL

The general arrangement of the model and curves showing the dead-
rise distribution for the three forebodies and three afterbodies are
shown in figure 1. The body plan is shown in figure 2. Forebody 1
and afterbody 1 form the basic model. In order to obtain the sections
for the other forebodies and afterbodies, the straight portion of each
section was rotated about the keel to the angle of dead rise shown in
figure 1. The local beam at the chine was kept constant and the chine
flare at each station was kept constant insofar as possible. The
forebody and afterbody keel profile, forebody and afterbody length,
step plan form and depth, and sternpost angle were left unaltered.

Preliminary tests showed that the afterbody chines did not
provide a sharp enough break to prevent the flow of water over the
sides of the afterbody and tail extension, and that the resistance
at the hump and high speeds was excessive. Similar behavior had been
observed during earlier tests of the basic model (reference 1).
Chine strips similar to those used in the tests of reference 1 were
therefore added to all the afterbodies. (See figs. 1 and 2.) The
following combinations were tested:

Forebody	Afterbody	Model number
1 (high dead rise at bow)	1 $\left(\text{max. dead rise at station } 17\frac{1}{2}\right)$	207A
2 (intermediate dead rise at bow)	1 $\left(\text{max. dead rise at station } 17\frac{1}{2}\right)$	207B
3 (low dead rise at bow)	1 $\left(\text{max. dead rise at station } 17\frac{1}{2}\right)$	207C
3 (low dead rise at bow)	2 (max. dead rise at station 19)	207D
3 (low dead rise at bow)	3 (max. dead rise at station 21)	207E

APPARATUS AND PROCEDURE

The tests were made in Langley tank no. 1, which is described
in reference 2. The free-to-trim resistance characteristics were
determined for all models to speeds beyond the hump. Fixed-trim
tests of model 207E were made at sufficient trims to include zero
trimming moment at hump speed and best trim from hump speed to
get-away speed. Fixed-trim tests of model 207D were discontinued
when the initial results showed no significant changes when compared
with those of model 207E. The air-flow conditions for the present
tests were slightly different from those for the original tests of
model 207A (reference 1), because of changes in the towing apparatus
and observation platform. The tests of the basic model, model 207A,
were therefore repeated in order to make the data directly comparable.

The center of gravity for the free-to-trim tests was located
12.25 inches above the straight portion of the forebody keel and
9.52 inches forward of the point of the vee step. Moments were
taken about this same point during the fixed-trim tests.

Tests were made at the normal gross load and at an arbitrarily
assumed overload. The gross loads investigated and the corresponding
get-away speeds are given in the following table:

Gross load			Get-away speed		
Full-size (lb)	$\frac{1}{11}$-size model (lb)	C_{Δ_0}	Full-size (ft/sec)	$\frac{1}{11}$-size model (ft/sec)	C_V
105,000	78.2	0.567	129.6	38.9	5.02
125,000	93.1	.675	141.6	42.5	6.58

The same unloading curves described in reference 1 and shown in
figure 3 were used for this investigation. The unloading curves
were calculated for an assumed C_L of 2.0 and a full-size wing
area of 2625 square feet.

Spray photographs were taken at low speeds to determine the
coordinates of the peaks of the bow-spray blisters with reference

to the model. Simultaneous bow and side photographs were taken at intervals of 2 feet per second from 6 to 16 feet per second for loads corresponding (to the nearest 0.025 C_Δ) to each of the unloading curves. Photographs of a grid were taken with both cameras, and all measurements of spray were corrected for parallax by means of these photographs. The results are plotted on profile and plan views of the model.

RESULTS AND DISCUSSION

The results of the free-to-trim and fixed-trim tests of model 207E are shown in figures 3 and 4. Model 207E represents the combination of forebody and afterbody with the greatest changes from the basic model (207A).

The effect of changes in dead rise at the bow on the free-to-trim characteristics is shown in figure 5 where results from the tests of models 207A, 207B, and 207C are compared. The effect of changes in the position of maximum dead rise of the warped afterbody on the free-to-trim characteristics is shown in figure 6 where results from the tests of models 207C, 207D, and 207E are compared. It can be seen from figures 5 and 6 that neither the changes in the amount of dead rise at the bow nor the changes in the position of maximum dead rise of the afterbody caused significant changes in the free-to-trim resistance or trim. The small resistance differences at high speed are not consistent and are within the accuracy of free-to-trim measurements.

In figure 7 fixed-trim data for models 207A and 207E (which have the greatest differences in forebody and afterbody dead rise) are compared at speed coefficients C_V of 4.2, 5.0, and 5.8. The resistance of model 207E appears to be slightly lower than that of model 207A, but the differences are too small to be significant. The trimming moments for the two models are the same.

The bow-spray photographs of model 207E are shown in figure 8. The effect of changes in dead rise at the bow on the height of the bow blister is shown in figure 9 where the coordinates of the peaks of the bow blisters are shown for models 207A (high dead rise at bow) and 207C (low dead rise at bow). Up to a speed coefficient of about 2.0 the model with the low dead rise at the bow had slightly lower bow blisters than the model with the high dead rise at the bow. At higher speeds the part of the forebody affected by the changes was out of the water and there were no differences in spray characteristics. The coordinates of the blister peaks for the model with intermediate dead rise at the bow, model 207B, were found to be consistently

intermediate to those for models 207A and 207C. A comparison of
figures 9(a) and 9(b) shows that for both models the heights of
the blisters increased with increase in gross load.

The coordinates of the blister peaks for models 207C and 207E
(same forebody and greatest differences in position of maximum dead
rise of afterbody) were compared and found to be identical. This
was to be expected since the changes in the position of the maximum
dead rise of the afterbody did not affect the trim at low speeds.

CONCLUSIONS

1. The variations in forebody and afterbody dead rise, within
the range investigated, caused no significant changes in resistance
or trim, free to trim, or in resistance or trimming moment,
fixed in trim.

2. The model with the low dead rise at the bow had the lowest
bow-spray blisters at low speeds. The changes in position of maximum
dead rise of the afterbody had no effect on the bow-spray blister.

Langley Memorial Aeronautical Laboratory
        National Advisory Committee for Aeronautics
                Langley Field, Va.

Eugene P. Clement
Naval Architect

Charles J. Daniels
Naval Architect

Approved: John B. Parkinson
John B. Parkinson
Chief of Hydrodynamics Division

BUB

REFERENCES

1. Woodward, David R., and Leventhal, Bernard E.: Resistance Tests
    of a 1/11-Size Model of the Hull of the Bureau of Aeronautics
    Design No. 22ADR Class VPB Airplane - Langley Tank Model 207 -
    TED No. NACA 2361. NACA MR No. L5H06a, Bur. Aero., 1945.

2. Truscott, Starr: The Enlarged N.A.C.A. Tank, and Some of Its
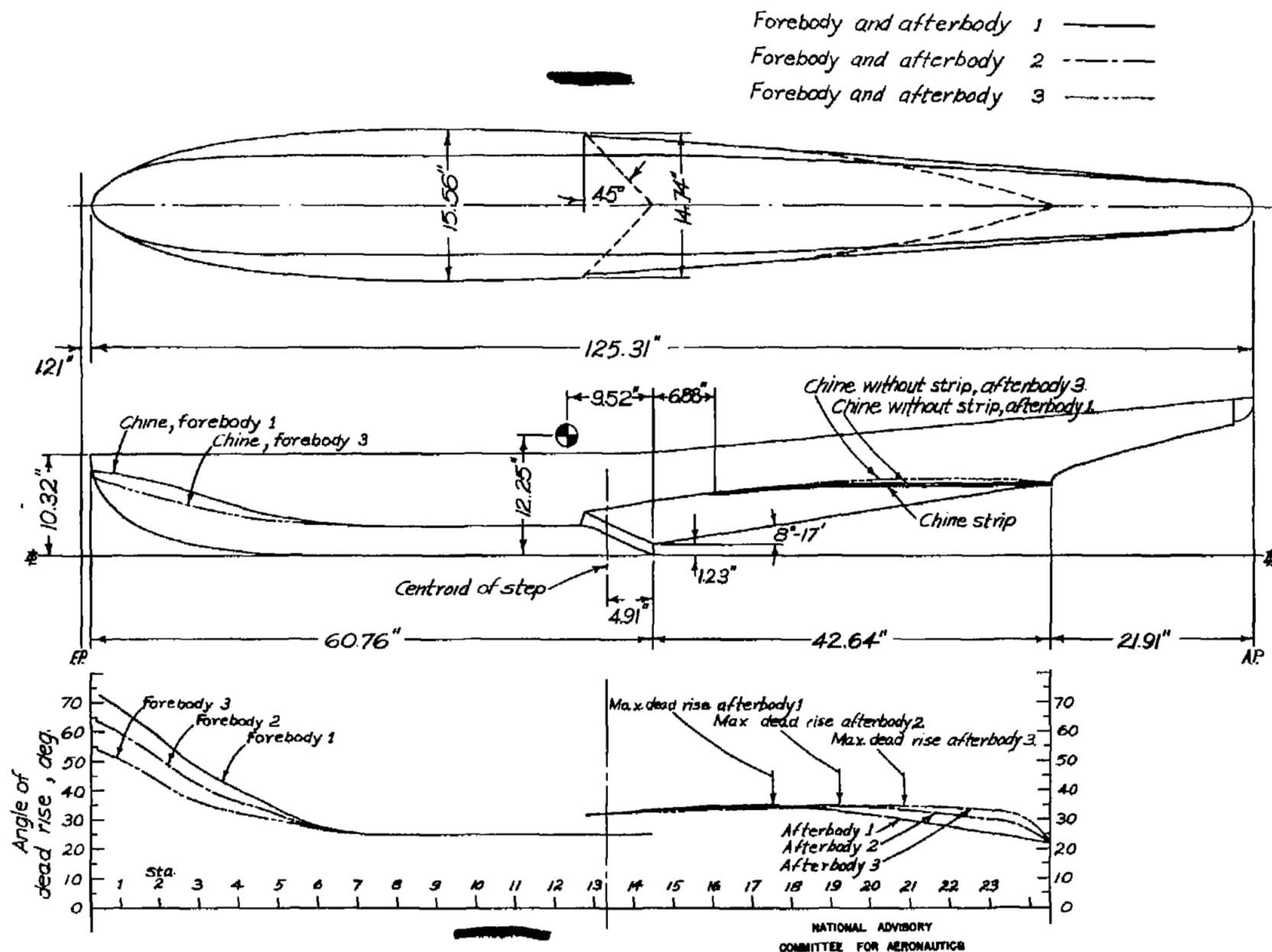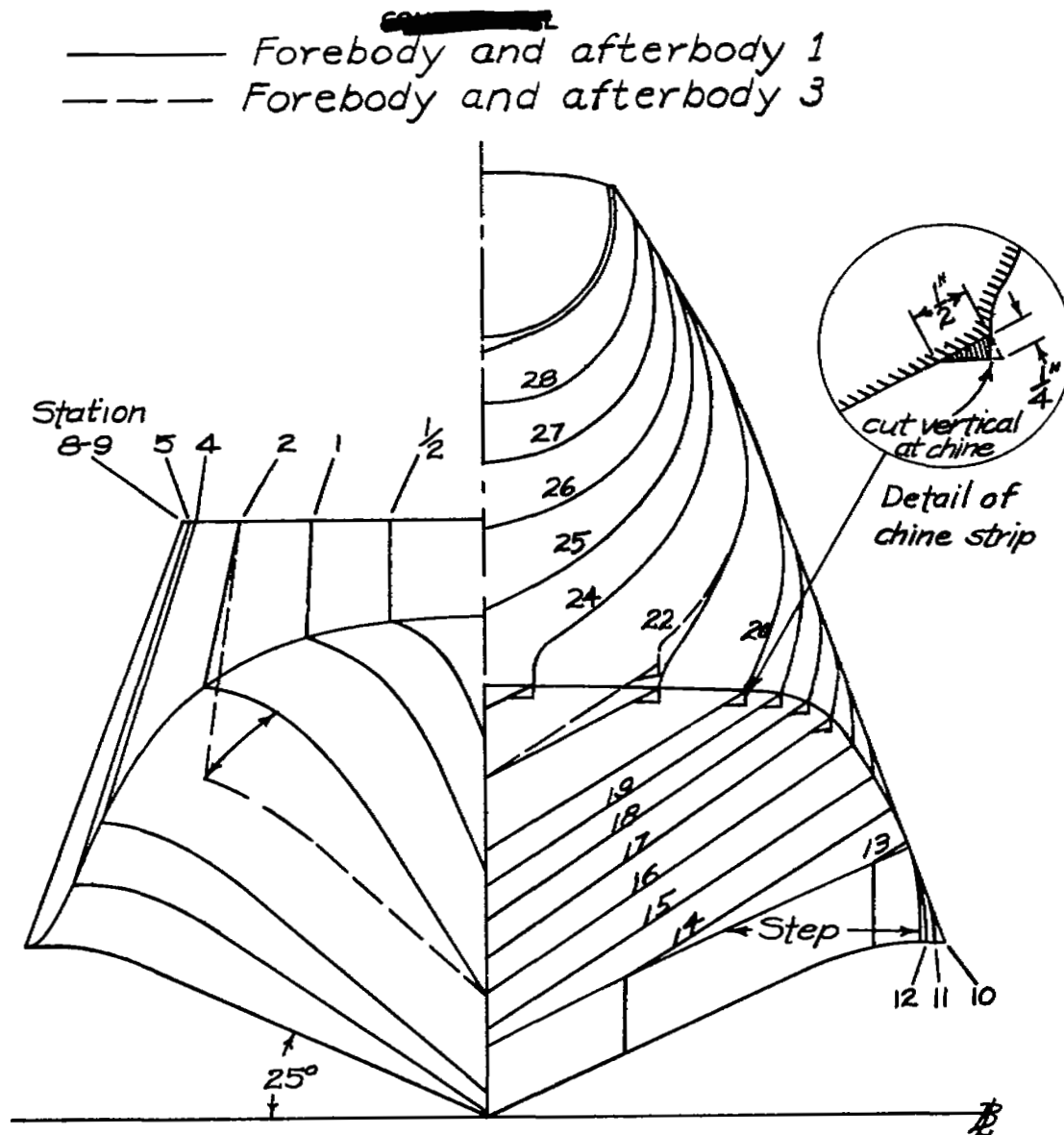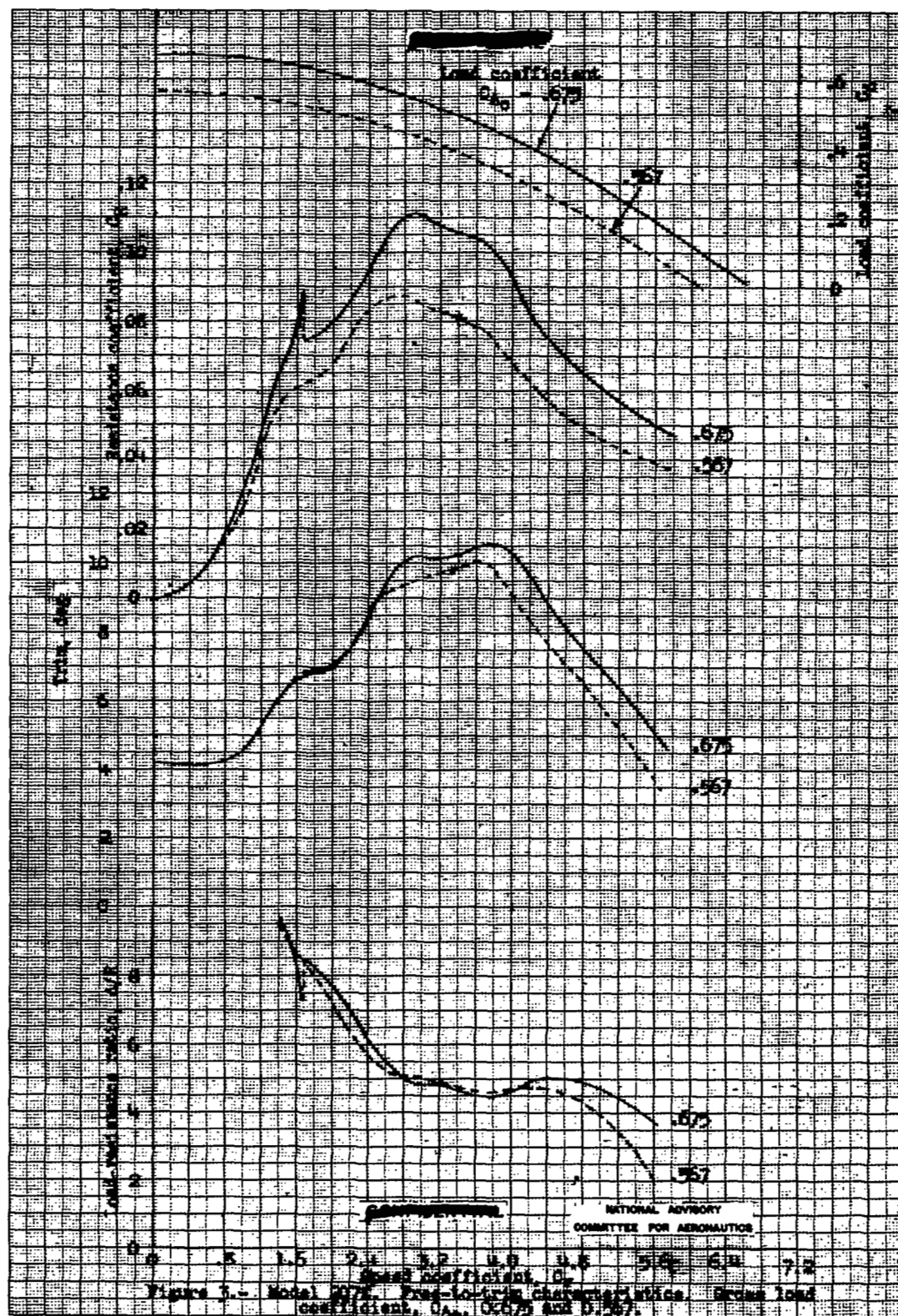   Work. NACA TM No. 918, 1939.

Forebody and afterbody 1 ————
Forebody and afterbody 2 —·—·—
Forebody and afterbody 3 ———···———

15.56"

45°

14.74"

121"

125.31"

9.52"

6.88"

Chine without strip, afterbody 3.
Chine without strip, afterbody 1.

Chine, forebody 1
Chine, forebody 3

10.32"

12.25"

Chine strip

8°-17'

1.23"

Centroid of step

4.91"

60.76"

42.64"

21.91"

F.P.

A.P.

Angle of dead rise, deg.

70
60
50
40
30
20
10
0

Forebody 3
Forebody 2
Forebody 1

Max. dead rise afterbody 1
Max. dead rise afterbody 2
Max. dead rise afterbody 3

Afterbody 1
Afterbody 2
Afterbody 3

70
60
50
40
30
20
10
0

sta.
1 2 3 4 5 6 7 8 9 10 11 12 13 14 15 16 17 18 19 20 21 22 23

Figure 1.– Model 207 series. General arrangement.

Fig. 1

—————— Forebody and afterbody 1
— — — — Forebody and afterbody 3

Station
8-9 5 4   2 1   ½

28
27
26
25
24
22   20

cut vertical
at chine

Detail of
chine strip

19
18
17
16
15
14   ←Step→

13

12 11 10

25°

Ɫ

Figure 2.—Model 207 series. Body plan.

Figure 3.- Model 307E. Free-to-trim characteristics. Gross load coefficient, C_{Δ_0}, 0.675 and 0.567.

(a) Gross load coefficient, C_{Δ_0}, 0.57

Figure 4.- Model 207E. Fixed Trim characteristics.

NATIONAL ADVISORY
COMMITTEE FOR AERONAUTICS

(b) Gross load coefficient, C_{Δ_0}, 0.675

Figure 4.- Concluded.
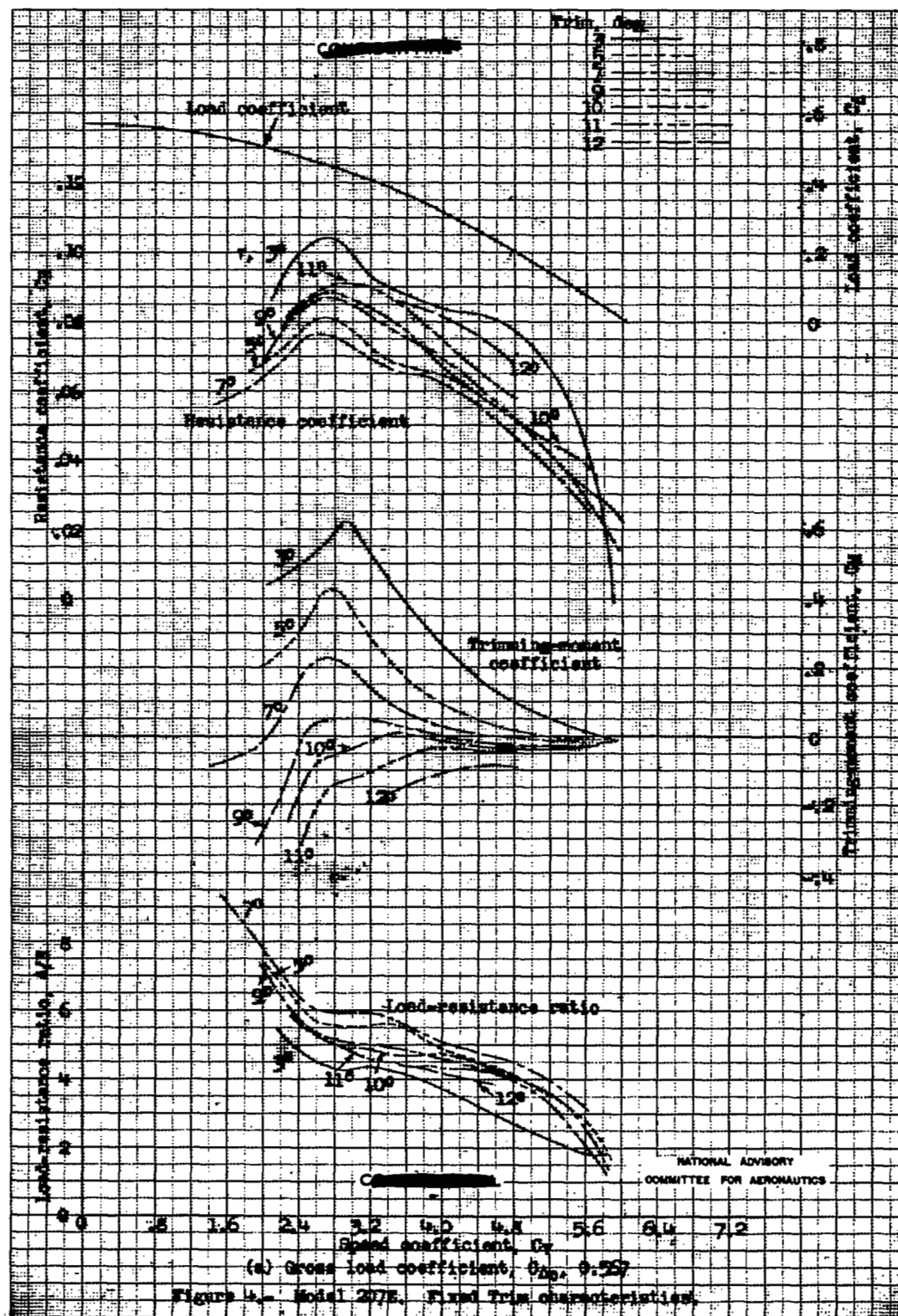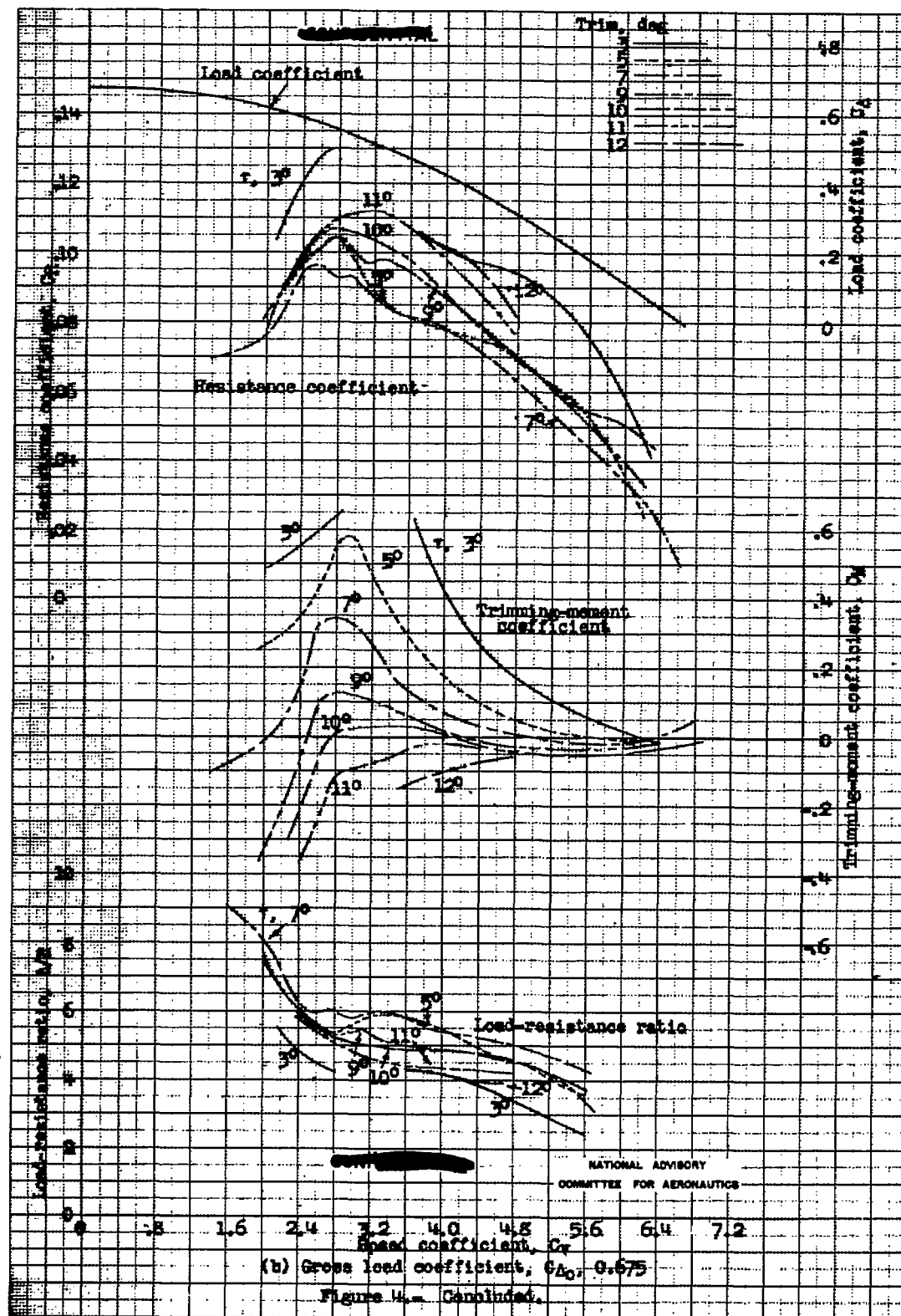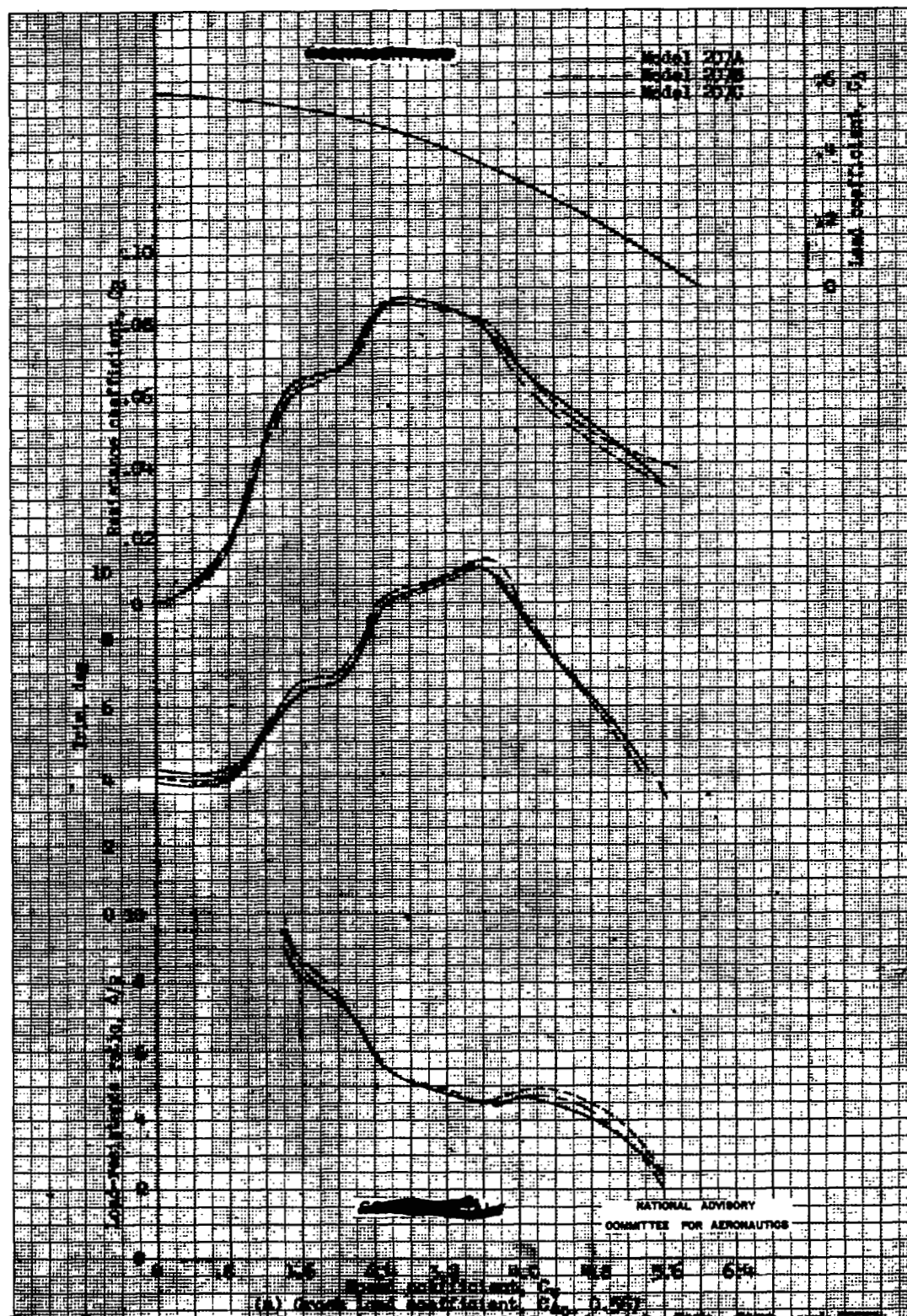
Figure 5.- Comparison of aerodynamic characteristics of models 207A, 207B, and 207C.

(b) Beam load coefficient, C_{Δ_0}, 0.675

Figure 5.- Concluded.

(a) Gross load coefficient, C_{Δ_0} 0.567

Figure 6.- Comparison of free-to-trim characteristics of models 207C, 207D, and 207E.

(b) Gross load coefficient, C_{Δ_0}, 0.675

Figure 6.— Concluded.

Figure 7.— Comparison of fixed-trim characteristics of models 207A and 207E for 3 planing speeds.

C_V, 0.93 C_Δ, 0.65 τ, 4.1°

C_V, 1.24 C_Δ, 0.65 τ, 5.2°
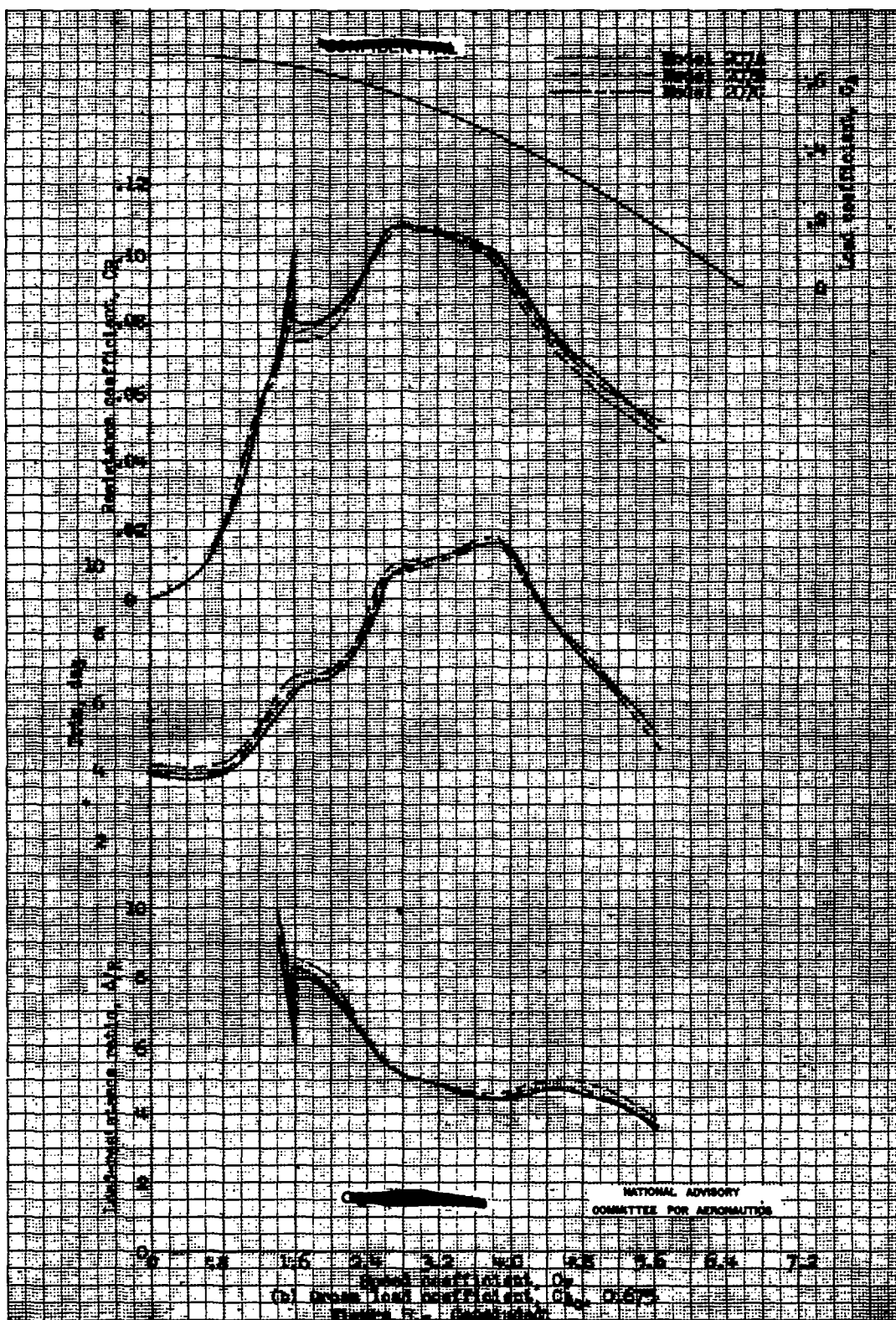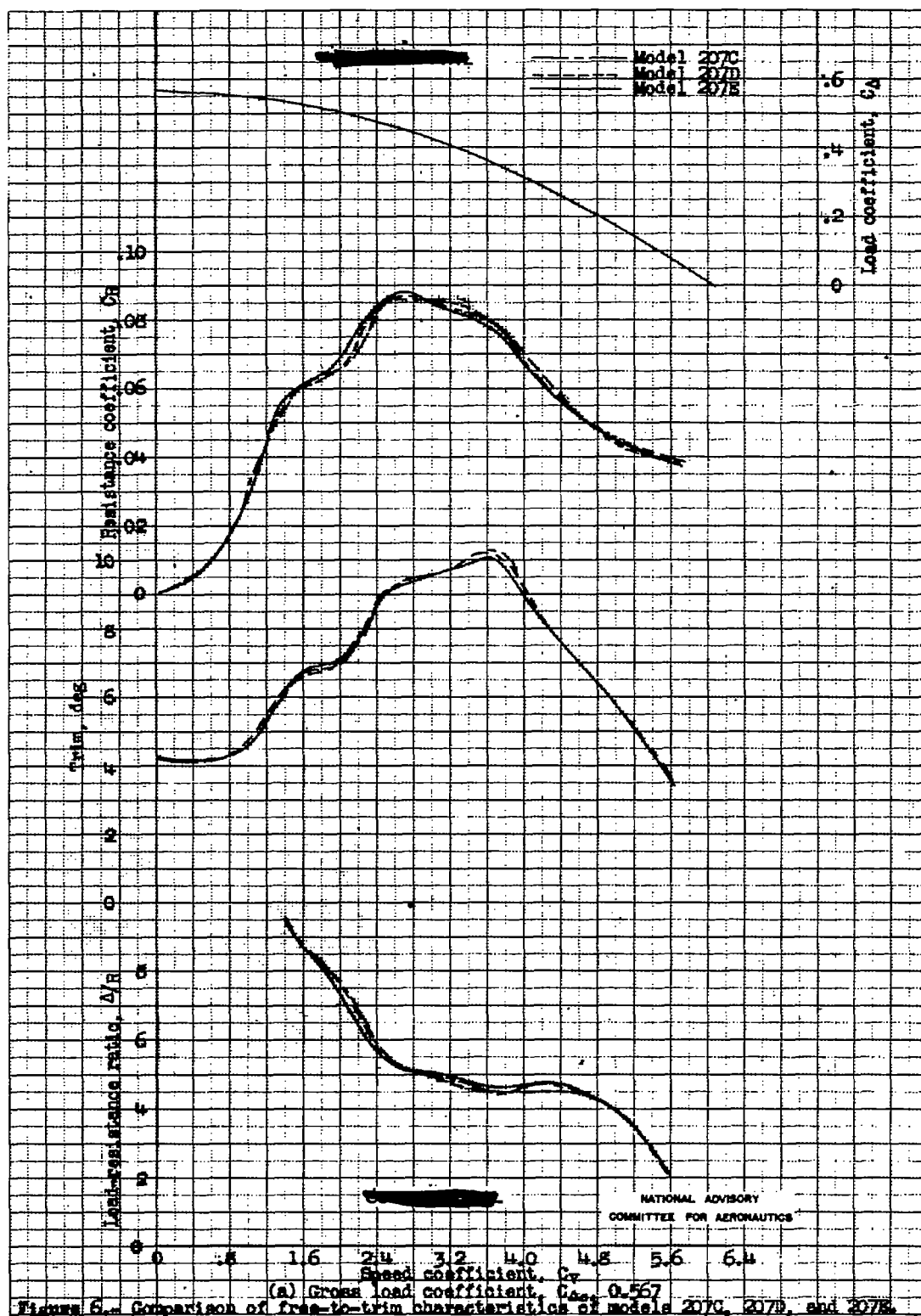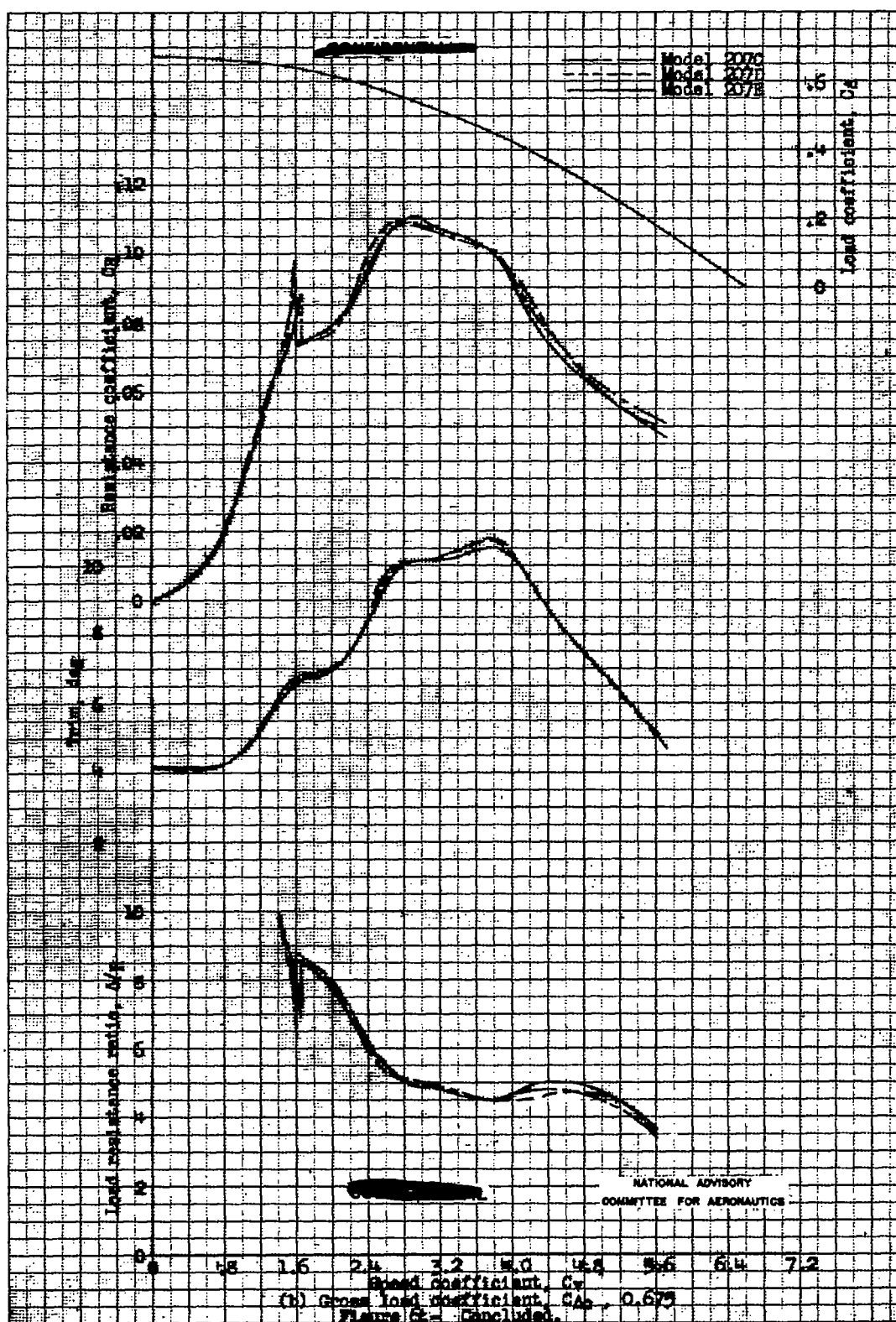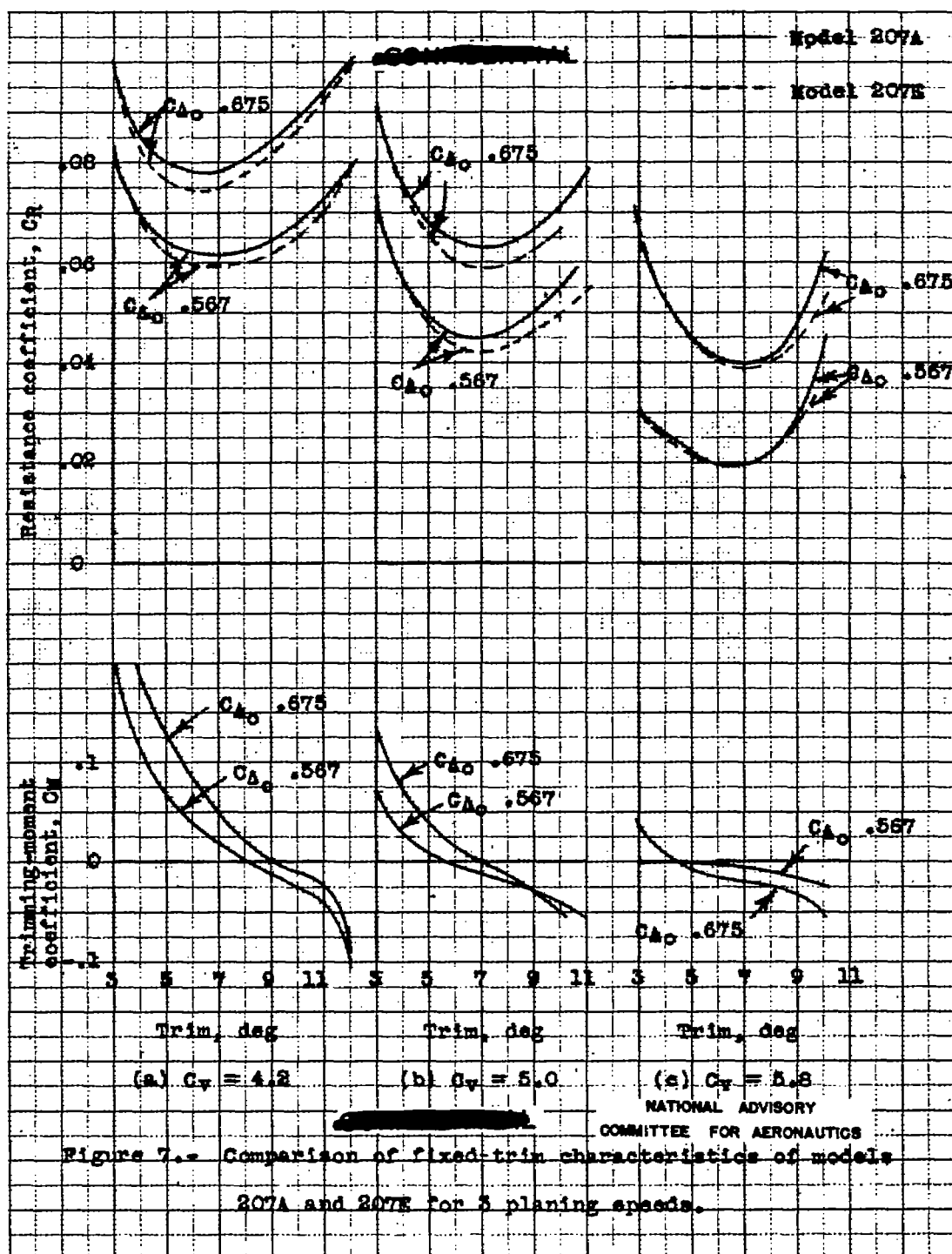
C_V, 1.55 C_Δ, 0.625 τ, 6.6°

Figure 8.-   Model 207E.   Bow-spray photographs, free-to-trim.
C_{Δ_0},   0.675.

C_V, 1.86 $\qquad$ C_Δ, 0.625 $\qquad$ τ, 6.8°

C_V, 2.17 $\qquad$ C_Δ, 0.60 $\qquad$ τ, 7.5°

C_V, 2.48 $\qquad$ C_Δ, 0.575 $\qquad$ τ, 9.2°

Figure 8.- Concluded.

Figure 9.- Coordinates of peaks of bow-spray blisters for models 207A and 207C.

(a) Gross load coefficient, C_Δo = 0.597.

Model 207A ———⊖———

Model 207C ——*——

Inboard propeller

C_V 95   1.25   1.86   2.17   2.46

Centroid of step

Inches, model size

NATIONAL ADVISORY
COMMITTEE FOR AERONAUTICS

(b) Gross load coefficient, C_{Δ_0}, 0.575.

Figure 9.- Concluded.